Europium(III) Complex Probing Distribution of Functions Grafted using Molecular Stencil Patterning in 2D Hexagonal Mesostructured Porous Silica

S. Abry,[†] F. Lux,[†] B. Albela,[†] A. Artigas-Miquel,[†] S. Nicolas,[†] B. Jarry,[†] P. Perriat,[‡] G. Lemercier,*[,†,§] and L. Bonneviot*[,†]

Université de Lyon, Laboratoire de Chimie, École Normale Supérieure de Lyon, CNRS 46, Allée d'Italie, 69364 Lyon Cedex 07, France, Université de Lyon, MATEIS, INSA-Lyon, CNRS 69621 Villeurbanne Cedex, France, Université de Reims Champagne-Ardenne, CNRS, ICMR, Moulin de la Housse BP 1039, 51687 Reims Cedex 2, France

Received October 9, 2008. Revised Manuscript Received April 3, 2009

The "molecular stencil patterning" technique has been used to optimize at high coverage the distribution of aminopropylsilyl tethers (APS) grafted into the nanochannels of a mesostructured MCM-41 type porous silica. To probe this distribution, the APS functions are first derivatized via a Schiff reaction with a 5-substituted 1,10-phenanthroline possessing an aldehyde side arm, and second, reacted with europium(III) ions used as a analytical marker. The integrity of the porous structure has been checked using XRD and N_2 adsorption−desorption profiles, whereas the molecular nature of the grafted Eu complex was characterized using ^{13}C NMR, FT-IR, reflectance UV−visible, and luminescence spectroscopies. EDX-TEM measurements at the 1.5 × 1.5 nm resolution scale reveal a rather homogeneous distribution of Eu and, therefore, of APS tethers for several micrometers inside the fibers.

Introduction

Immobilization of guest species into well-defined pores of inorganic solids has recently been investigated to design functional supramolecular materials where confinement is combined with specific function. For example, transition-metal complexes can be incorporated on various supports such as mesostuctured porous materials to obtain new types of heterogeneous catalysts where high dispersion of sites is combined with controlled accessibility.[1−7] Among metals of particular interest, rare-earth ions can give rise to a variety of applications not only for catalytic purposes[8,9] but also in magnetic resonance imaging (MRI)[10−12] and for a wide range of photophysical studies[13,14] (organic light-emitting diodes,[15,16] solid-state lasers,[17,18] optical communications,[19] and in drug delivery systems[20]). Optimization of the chemical and physical properties is always a challenge. Indeed, clustering, inhomogeneous dispersion, and leaching of the complexes may occur during synthesis or aging of the material. To minimize these negative effects and to improve the robustness of the material, covalent fixation to the backbone of the network is preferred to van der Waals interactions and hydrogen-bonding types of linkage.

Despite many examples of highly dispersed organic or metallic functions in porous solid matrices[21−24] (alumina, silica, alumino-silicate, titania, graphite), implementing both short and long-range homogeneities in the dispersion of covalently fixed species inside the mesopores of a solid remains an open challenge. Usually, grafting species on a preformed support requires low concentration and long contact time to prevent concentration gradient due to

* Corresponding author. E-mail: laurent.bonneviot@ens-lyon.fr.
† Université de Lyon, Laboratoire de Chimie.
‡ Université de Lyon, MATEIS.
§ Université de Reims Champagne-Ardenne.

(1) Gates, B. C. *Chem. Rev.* **1995**, *95*, 511–522.
(2) Corma, A. *Chem. Rev.* **1997**, *97*, 2373–2419.
(3) Moller, K.; Bein, T. *Chem. Mater.* **1998**, *10*, 2950–2963.
(4) Stein, A. *Adv. Mater.* **2003**, *15*, 763–775.
(5) Baute, D.; Arieli, D.; Neese, F.; Zimmermann, H.; Weckhuysen, B. M.; Goldfarb, D. *J. Am. Chem. Soc.* **2004**, *126*, 11733–11745.
(6) Taguchi, A.; Schueth, F. *Microporous Mesoporous Mater.* **2005**, *77*, 1–45.
(7) Mesu, J. G.; Visser, T.; Beale, A. M.; Soulimani, F.; Weckhuysen, B. M. *Chem.—Eur. J.* **2006**, *12*, 7167–7177.
(8) Parac-Vogt, T. N.; Pachini, S.; Nockemann, P.; Van Hecke, K.; Van Meervelt, L.; Binnemans, K. *Eur. J. Org. Chem.* **2004**, *456*, 0–4566.
(9) Gandara, F.; Perles, J.; Snejko, N.; Iglesias, M.; Gomez-Lor, B.; Gutiérrez-Puebla, E.; Monge, M.-A. *Angew. Chem., Int. Ed.* **2006**, *45*, 7998–9001.
(10) Zhang, S.; Wu, K.; Biewer, M. C.; Sherry, A. D. *Inorg. Chem.* **2001**, *40*, 4284–4290.
(11) Nonat, A. H.; Fries, P.; Pécaut, J.; Mazzanti, M. *Chem.—Eur. J.* **2007**, *13*, 8489–8506.
(12) Giardiello, M.; Lowe, M. P.; Botta, M. *Chem. Comm.* **2007**, 4044–4046.
(13) Bünzli, J.-C. G.; Comby, S.; Chauvin, A.-S.; Vandevyver, C. D. B. *J. Rare Earth* **2007**, *25*, 257–274.
(14) Chen, X.-Y.; Bretonnière, Y.; Pécaut, J.; Imbert, D.; Bünzli, J.-C.; Mazzanti, M. *Inorg. Chem.* **2007**, *46*, 625–637.
(15) Kido, J.; Okamoto, Y. *Chem. Rev.* **2002**, *102*, 2357–2368.
(16) Fang, J.; You, H.; Gao, J.; Lu, W.; Ma, D. *J. Lumin.* **2007**, *124*, 157–161.
(17) Marlow, F.; McGehee, M. D.; Zhao, D.; Chmelka, B. F.; Stucky, G. D. *Adv. Mater.* **1999**, *11*, 632–636.
(18) Besson, E.; Mehdi, A.; Matsura, V.; Guari, Y.; Rey, C.; Corriu, R. J. P. *Chem. Commun.* **2005**, 1775–1777.
(19) Bunzli, J.-C. G.; Piguet, C. *Chem. Rev.* **2002**, *102*, 1897–1928.
(20) Yang, P.; Huang, S.; Kong, D.; Lin, J.; Fu, H. *Inorg. Chem.* **2007**, *46*, 3203–3211.
(21) Hicks, J. C.; Jones, C. W. *Langmuir* **2006**, *22*, 2676–2681.
(22) Wulff, G.; Heide, B.; Helfmeier, G. *J. Am. Chem. Soc.* **1986**, *108*, 1089–1091.
(23) Tahmassebi, D. C.; Sasaki, T. *J. Org. Chem.* **1994**, *59*, 679–681.
(24) Wight, A. P.; Davis, M. E. *Chem. Rev.* **2002**, *102*, 3589–3613.

10.1021/cm802752r CCC: $40.75
Published on Web 05/27/2009

diffusion-controlled processes.[25−28] It is worth noting that diffusion is important in nanoscale channels and depends on the structure, the morphology of the grains, and the pore network. At best, the dispersion relies on statistical distribution.[29]

To prevent concentration profile, one may synthesize the solid via soft chemistry, directly including the specific species X to be immobilized. For silica inorganic type of matrix, the sol−gel should contain a mixture of silica precursors to force the location of the organic species in the pore wall.[30] Organic species X at relatively high concentration can be incorporated in the solid up to a level where they are more than a simple host and formally take part of the solid structure and stability. This so-called co-condensation route should in principle lead to statistical distribution of the species inside the solid. This strategy is limited to very specific conditions depending on the nature and the stability of the immobilized species. In addition, the reactant accessibility to the sites is a problem to solve in each case. To the best of our knowledge, there are few examples of metal complex immobilization following this approach. One may cite cyclam- and amino-based coordination complexes[31−33] or rhodium and platinum catalytically active organometallic species, stabilized in SBA-3 mesostructured silica.[34,35]

The simplest and most-used route for function fixation remains the postgrafting under investigation here. To treat the specific problem of local aggregation during the grafting of propylaminosilanes, Jones et al. have proposed the use of steric hindrance via a large protecting group allowing vicinal distance control at low or high surface coverage.[36] Using this technique, Ti and Zr organometallic sites were successfully isolated and applied in ethylene polymerization.[37,38] Alternatively, the site isolation can be forced using the grafting of long chain silanes in between specific adsorption sites.[39] Another type of approach proposed by Anwander et al. consists of taking advantage of the grafting mechanism of highly reactive species (organo-rare-earths) to isolate the sites one to another.[40−42] The fixation of the metal to the oxide surface through cleavage of some of the metal−carbon bonds occurs concomitantly with both siloxane bridge opening and alkylation of the vicinal silicon groups. This favors site isolation and control over the site molecular vicinity. Alternatively, the use of silazanes has been developed by the same group to yield such local environment for multifunctionalisation.[43,44] This self-protected grafting method needs highly dehydrated silicas. Both routes are not universal because site unicity and site isolation require specific conditions depending on the nature and the reactivity of the grafted species. Furthermore, the latter approach is diffusion controlled and likely to produce long-range inhomogeneity, whereas the former circumvent this problem only for full coverage. To cope with this problem, a novel technique for site isolation and for homogeneous distribution of the functions has been proposed by some of us and called "molecular stencil patterning" (MSP).[45,46] The surface is fully covered by two functions, using the first one to dilute the second one according to a sequential grafting process. The surfactant, which is maintained in the templated silica at a controlled level of concentration, plays the role of protecting agent for a part of the surface silanol groups during the grafting of the first function, a timethylsilyl group (TMS). The surfactant is then removed in reaction conditions that retain the grafted TMS groups. The second function, a (mono- or tri-) ethoxy- or trichloro-organosilane, is then grafted without displacing the first one. The patterning effect is arising from self-repulsion between the positively charged heads of the surfactant during the fixation of the first function. Using this technique, highly reactive isothiocyanate groups can be grafted and further derivatized with a high yield on such a silanol-rich surface thanks to the protecting role of the first function, the grafting of which can be seen as a precapping step.[47] In addition, a combined EPR and extended X-ray absorption fine structure (EXAFS) study of some of us shows that molecular stencil patterning can lead to site isolation and prevent grafted Cu(II) complexes from pairing one to another at relatively high copper loading of ca. 3 wt %.[48−50] Although both site protecting and isolation effects of the MSP technique have been studied, no investigation of the long-range distribution of the function at the micrometer scale length has been yet performed.

(25) Lim, M. H.; Stein, A. *Chem. Mater.* **1999**, *11*, 3285–3295.
(26) Yokoi, T.; Yoshitake, H.; Tatsumi, T. *J. Mater. Chem.* **2004**, *14*, 951–957.
(27) Meynen, V.; Segura, Y.; Mertens, M.; Cool, P.; Vansant, E. F. *Microporous Mesoporous Mater.* **2005**, *85*, 119–128.
(28) Kim, H. J.; Ahn, J. E.; Haam, S.; Shul, Y. G.; Song, S. Y.; Tatsumi, T. *J. Mater. Chem.* **2006**, *16*, 1617–1621.
(29) Stempniewicz, M.; Khalil, A. S. G.; Rohwerder, M.; Marlow, F. *J. Am. Chem. Soc.* **2007**, *129*, 10561–10566.
(30) Hoffmann, F.; Cornelius, M.; Morell, J.; Froba, M. *Angew. Chem., Int. Ed.* **2006**, *45*, 3216–3251.
(31) Dubois, G.; Corriu, R. J. P.; Reyé, C.; Brandes, S.; Denat, F.; Guilard, R. *Chem. Commun.* **1999**, *22*, 2283–2284.
(32) Karakassides, M. A.; Bourlinos, A.; Petridis, D.; Coche-Guerente, L.; Labbe, P. *J. Mater. Chem.* **2000**, *10*, 403–408.
(33) Corriu, R. J. P.; Mehdi, A.; Reyé, C.; Thieuleux, C. *Chem Commun.* **2003**, *13*, 1564–1565.
(34) Dufaud, V.; Beauchesne, F.; Bonneviot, L. *Angew. Chem., Int. Ed.* **2005**, *44*, 3475–3477.
(35) Crowther, N. PhD Thesis. École Normale Supérieure de Lyon, Lyon University, Lyon, France, 2007.
(36) McKittrick, M. W.; Jones, C. W. *Chem. Mater.* **2003**, *15*, 1132–1139.
(37) Yu, K. Q.; McKittrick, M. W.; Jones, C. W. *Organometallics* **2004**, *23*, 4089–4096.
(38) McKittrick, M. W.; Jones, C. W. *J. Am. Chem. Soc.* **2004**, *126*, 3052–3053.
(39) Shin, Y. S.; Liu, J.; Wang, L. Q.; Nie, Z. M.; Samuels, W. D.; Fryxell, G. E.; Exarhos, G. J. *Angew. Chem., Int. Ed.* **2000**, *39*, 2702–2707.
(40) Nagl, I.; Widenmeyer, M.; Grasser, S.; Kohler, K.; Anwander, R. *J. Am. Chem. Soc.* **2000**, *122*, 1544–1545.
(41) Nagl, I.; Widenmeyer, M.; Herdtweck, E.; Raudaschl-Sieber, G.; Anwander, R. *Microporous Mesoporous Mater.* **2001**, *44*, 311–319.
(42) Anwander, R. *Chem. Mater.* **2001**, *13*, 4419–4438.
(43) Anwander, R.; Nagl, I.; Widenmeyer, M.; Engelhardt, G.; Groeger, O.; Palm, C.; Roser, T. *J. Phys. Chem. B* **2000**, *104*, 3532–3544.
(44) Zapilko, C.; Widenmeyer, M.; Nagl, I.; Estler, F.; Anwander, R.; Raudaschl-Sieber, G.; Groeger, O.; Engelhardt, G. *J. Am. Chem. Soc.* **2006**, *128*, 16266–16276.
(45) Abry, S.; Albela, B.; Bonneviot, L. *C. R. Chimie* **2005**, *8*, 741–752.
(46) Badiei, A.; Bonneviot, L.; Crowther, N.; Ziarani, G. M. *J. Organomet. Chem.* **2006**, *691*, 5911–5919.
(47) Calmettes, S.; Albela, B.; Hamelin, O.; Ménage, S.; Miomandre, F.; Bonneviot, L. *New J. Chem.* **2008**, *32*, 727–732.
(48) Abry, S.; Zhang, P.; Albela, A.; Bonneviot, L. *Stud. Surf. Sci. Catal.* **2007**, *107*, 1781–1787.
(49) Abry, S.; Thibon, A.; Albela, A.; Delichère, P.; Banse, F.; Bonneviot, L. *New J. Chem.*, **2009**, *33*, 484–496.
(50) Abry, S. PhD Thesis. École Normale Supérieure de Lyon, Lyon University, Lyon, France, 2007.

In this study, europium, a phosphorescent and heavy metal, is used not only as a probe of coordination symmetry and intermolecular distance, but also as an analytical marker for energy-dispersive X-ray (EDX) analysis to study the distribution of grafted functions at long-range scale of length. For comparison with the present work, there are several studies reporting on lanthanide complexes introduced inside the channel of MCM-48[51] and MCM-41[52,53] silicas by ion exchange. Of particular interest, one of them deals with the Eu-$(Phen)_2Cl_3(H_2O)_3$ complex (Phen for 1,10-phenanthroline),[54,55] the structure of which has been lately investigated by some of us.[56] Recently, one-pot synthesis of mesostructured silica thin films in which lanthanide complexes were covalently retained into the silica framework have also been reported; however, porous mesostructuration and species localization are still unresolved.[57] Apparently, the coordination properties may change in such systems. For instance, europium can form a complex with a tetradentate amino ligand in SBA-15, whereas it does not in pure water.[58] Therefore, the coordination state of the europium ion has to be monitored with special care in such siliceous matrices. In addition, thanks to the relatively high atomic mass *Z* of rare-earth elements, the use of EDX appears an adequate technique to monitor the concentration profile on the elements in the grains or the fibers of the material.[59] Though 3D EDX imaging is already available,[60] a point-by-point analysis is better suited for nano-objects at high resolution.[61,62] To the best of our knowledge, the present study is the first of this kind that achieves local analysis at such a high resolution as announced in the abstract.

Here, both properties of Eu(III) are used to probe molecular site definition and distribution generated by the MSP technique. This ion is immobilized thanks to a covalently grafted ligand, a 1,10-phenanthroline derivative that contains an aldehyde side arm. The latter is reacted with an aminopropylsiloxane previously grafted onto the internal surface according to the MSP technique. Eu(III) is then complexed to the so-obtained immobilized ligand. It is worth noting that Phen is a weak ligand for Eu(III) that does not retain this ion irreversibly. In general, O-donor groups are much better ligands for lanthanides than 1,10-phenanthroline, even though the latter have to be associated together in cryptand system to efficiently trap lanthanide ions as shown for MRI applications.[63−66] However, the choice of a stronger ligand here would be a problem, generating entrance blockage and a poor probing capacity of europium for the overall ligand distribution all through the solid. A panel of techniques is applied to monitor each step of this "ship-in-the-bottle design" synthesis. A fluorescence lifetime study and a detailed TEM coupled EDX analysis of Eu(III) concentration along fibers are performed to probe the metal distribution at different scale of lengths.

Experimental Section

Physical Measurements. ^1H and ^{13}C NMR spectra were recorded on a Bruker DPX 200 spectrometer (at 200.13 MHz for ^1H and 50.32 MHz for ^{13}C) and also on a Varian Unity Plus at 499.84 MHz for ^1H, data being listed in parts per million (ppm) relative to tetramethylsilane. Elemental analyses were carried out by the "Service Central d'Analyse de Solaize", CNRS. Eu analysis has been performed at IRCE Lyon as follow: solids have been digested in a mixture of H_2SO_4, HNO_3 and HF, then evaporated to dryness, and finally redissolved in HNO_3 for analysis using ICP. ^{13}C CP-MAS solid NMR measurements were collected on a Bruker DSX300 spectrometer using a Bruker CP MAS 4 mm rotor. A contact time of 2 ms and a RD = 2 s were used. The spinning rate of the rotor was about 10 kHz. UV/vis spectra were recorded in the 200−800 nm range on a UV/vis Jasco V-550; λ_{max} are given in nm and molar extinction coefficients ε in L mol^{-1} cm^{-1}. Solid UV−visible and near-infrared spectra were recorded from aluminum cells with Suprasil 300 quartz windows, using a Perkin-Elmer Lambda 950 and PE Winlab software. The luminescence spectra were recorded on a Jobin-Yvon Fluoromax-2 spectrofluorimeter equipped with a red-sensitive Hamamatsu R928 photomultiplier tube. The emission spectra were corrected for the wavelength dependence of the PMT/emission monochromator by application of a correction curve generated from a standard lamp. The luminescence lifetimes were measured by multichannel scan, with data being collected over 2 ms at 1 μs/channel or over 4 ms at 2 μs/channel, following excitation with a xenon flashlamp operating at 100 Hz (pulse length of 2 μs). Melting temperatures mp were measured on a Perkin-Elmer DSC7 microcalorimeter. Low-angle X-ray powder diffraction experiments have been carried out using a Bruker (Siemens) D5005 diffractometer using Cu Kα monochromatic radiation. Infrared spectra were recorded from KBr pellets using a Mattson 3000 IRTF spectrometer. Quantification of the IR band at 850 cm^{-1} was performed as previously reported using the scissor deformation vibrational mode of the $[SiO_4]$ unit as an internal reference for inorganic silicon.[47] Nitrogen adsorption−desorption isotherms at 77 K were determined with a volume device Micromeritics ASAP 2010M. Adsorbed volumes are reported in standard temperature and pressure (STP) of gas equivalent on figure and in liquid equivalent corresponding to real volume in the text. TGA measurements were collected from Al_2O_3 crucibles on a DTA-

(51) Meng, Q. G.; Boutinaud, P.; Franville, A.-C.; Zhang, H. J.; Mahiou, R. *Microporous Mesoporous Mater.* **2003**, *65*, 127–136.
(52) Xu, Q.; Li, L.; Liu, X.; Xu, R. *Chem. Mater.* **2002**, *14*, 549–555.
(53) Gago, S.; Fernandes, J. A.; Rainho, J. P.; Sà Ferreira, R. A.; Pillinger, M.; Valente, A. A.; Santos, T. M.; Carlos, L. D.; Ribeiro-Claro, P. J. A.; Gonçalves, I. S. *Chem. Mater.* **2005**, *17*, 5077–5084.
(54) Li, H.; Inoue, S.; Machida, K.; Adachi, G. *J. Lumin.* **2000**, *87−89*, 1069–1072.
(55) Guo, X.; Fu, L.; Zhang, H.; Carlos, L. D.; Peng, C.; Guo, J.; Yu, J.; Deng, R.; Sun, L. *New J. Chem.* **2005**, *29*, 1351–1358.
(56) Raynaud, C.; Lux, F.; Lemercier, G.; Bonneviot, L.; Maron, L. *Inorg. Chem.* **2009**, in revision; it contains EXAFS, UV-visible, FT-IR, and luminescence spectroscopic investigations of $Eu(Phen)_2Cl_3(H_2O)_3$. Note that a nitrogen from a imino-group or an oxygen from a water molecule would hardly be differentiated by EXAFS.
(57) Li, H. R.; Zhang, H. J.; Fu, L. S.; Meng, Q. G.; Wang, S. B. *Chem. Mater.* **2002**, *14*, 3651–3655.
(58) Corriu, R. J. P.; Mehdi, A.; Reyé, C.; Thieuleux, C.; Frenkel, A.; Gibaud, A. *New J. Chem.* **2004**, *28*, 156–160.
(59) Markewitz, A. *Nucl. Instrum. Methods Phys. Res., Sect. B* **2000**, *161*, 221–226.
(60) Beale, A. M.; Jacques, S. D. M.; Bergwerff, J. A.; Barnes, P.; Weckhuysen, B. M. *Angew. Chem., Int. Ed.* **2007**, *46*, 8832–8835.
(61) Deki, S.; Iizuka, S.; Mizuata, M.; Kajinami, A. *J. Electroanal. Chem.* **2005**, *584*, 38–43.
(62) Chen, H. M.; MacDonald, R. C.; Li, S. Y.; Krett, N. L.; Rosen, S. T.; O'Halloran, T. V. *J. Am. Chem. Soc.* **2006**, *128*, 13348–13349.
(63) Zhang, S.; Wu, K.; Biewer, M. C.; Sherry, A. D. *Inorg. Chem.* **2001**, *40*, 4284–4290.
(64) Chen, X.-Y.; Bretonnière, Y.; Pécaut, J.; Imbert, D.; Bünzli, J.-C.; Mazzanti, M. *Inorg. Chem.* **2007**, *46*, 625–637.
(65) Bünzli, J.-C. G.; Comby, S.; Chauvin, A.-S.; Vandevyver, C. D. B. *J. Rare Earth* **2007**, *25*, 257–274.
(66) Giardiello, M.; Lowe, M. P.; Botta, M. *Chem. Commun.* **2007**, 4044–4046.

TG Netzsch STA 409 PC/PG instrument, under air (30 mL/min), with a 298−1273K (10 K/min) temperature increase. Imaging and analytical studies were performed on a JEOL 2010F microscope equipped with a field emission gun and operating at 200 kV. EDX (energy-dispersive X-ray analysis) was performed thanks to a dispersive X-ray system (INCA-Oxford equipment) with a detector owing a polymer ultrathin window. Local quantitative analyses were made according to the ZAF method (Z for atomic number correction accounting for electrons backscattering, A for absorption correction, and F for secondary fluorescence correction) using the ZAF's factors contained in the INCA software. Required data are the thickness and the volume mass of the analyzed zones. Systematically, the chosen value for thickness was the diameter of the fiber (the analysis being performed in the middle of the fiber), and the chosen volume mass was that of the silica. It was verified that these values have only a small influence on the results (maximal variation of 0.1% for relative thickness and volume mass variations of 10%).

Materials. Hexadecyltrimethylammonium-*p*-toluene-sulfonate (CTATos) (>99% Merck), hexamethyldisilazane (HMDSA) (98% Acros), Ludox HS-40 (40% SiO_2 Aldrich), and 3-aminopropyltriethoxysilane (APTES) (97% Aldrich) were used as received. Toluene, cyclohexane, acetonitrile and dichloromethane were stored with molecular sieve under argon. Preparation of $Eu(1,10\text{-}Phen)_2Cl_3(H_2O)_3$ has already been described elsewhere.[56] Synthesis of IBX reagent has been realized according to a previously reported method.[67] Preparative flash chromatography was performed on Merck Gerduran 60.

5-(but-3-yn-1-ol)-1,10-phenanthroline **1**. To a solution of 1 g of 5-bromo-1,10-phenanthroline (3.86 mmol) in 30 mL of pyrrolidine and under an inert atmosphere were added 350 μL of but-3-yn-1-ol (4.63 mmol) and 223 mg of tetrakis(triphenylphosphine)-palladium(0) (0.193 mmol). The eaction mixture was then warmed overnight at 70 °C and poured in 50 mL of a saturated NH_4Cl solution. Aqueous layer was extracted with 3 × 50 mL of dichloromethane and the resulting organic phases were washed with 3 × 25 mL of a saturated NH_4Cl solution being dried over Na_2SO_4 and evaporated to dryness. The crude black oil obtained was purified by column chromatography, eluting with pentane/CH_2Cl_2/NH_4OH (95/9.5/0.5) to lead to 564 mg of a beige solid (58% yield). Mp = 188 °C. ^{1}H NMR (200.13 MHz; $CDCl_3$): δ 9.19 (1H, dd, H_2 or H_9, J = 4.3; 1.7 Hz), 9.15 (1H, dd, H_9 or H_2, J = 4.3; 1.7 Hz), 8.70 (1H, dd, H_4 or H_7, J = 8.3; 1.7 Hz), 8.16 (1H, dd, H_7 or H_4, J = 8.3; 1.7 Hz), 7.94 (1H, s, H_6), 7.70 (1H, dd, H_3 or H_8, J = 8.3; 4.3 Hz), 7.60 (1H, dd, H_8 or H_3, J = 8.2; 4.3 Hz), 3.96 (2H, t, H_{14}, J = 6.1 Hz), 2.86 (2H, t, H_{13}, J = 6.2 Hz), 1.67 (1H, m, H_{15}, J = 5.8). ^{13}C NMR (50.32 MHz; $CDCl_3$): δ 151.4, 151.2, 146.6, 146.5, 136.3, 135.3, 131.2, 129.1, 128.6, 124.0, 123.9, 120.7, 93.7, 79.5, 61.8, 24.7. IR (KBr): $\nu_{CH\ aro}$ = 3110, 3086, 3056 cm^{-1}, νC_{sp} = 2232 cm^{-1}, $\nu_{C=C\ aro}$ = 1595, 1570, 1510, 1426 cm^{-1}, δ_{OH} = 1377 cm^{-1}, ν_{C-O} = 1065 cm^{-1}, δCH $_{aro}$ = 740 cm^{-1}. UV/vis (CH_2Cl_2) λ_{max} (ε): 210 (22200); 236 (34800); 272 (31100); 302 (11700); 312 (10700). Anal. Calcd for $C_{16}H_{12}N_2O_1$, 1 H_2O: C, 72.17; H, 5.30; N, 10.52%. Found: C, 72.62; H, 4.93; N, 10.66%.

5-(butan-1-ol)-1,10-phenanthroline **2**. In an autoclave, 0.47 g of 5-(but-3-yn-1-ol)-1,10-phenanthroline **1** (1.89 mmol) and 0.32 g of 10% Pd/C were dissolved in a mixture of 32 mL of methanol and 3.2 mL of 10% HCl_{aq}. The reaction mixture was then stirred for a night at room temperature under 20 bar pressure hydrogen atmosphere. The resulting red solution was filtred on Celite and concentrated before to be neutralized with a sodium hydroxide solution. After several extractions with chloroform, the organic layer was dried over Na_2SO_4. Filtration and evaporation to dryness led to 570 mg of a brown powder. Purification by column chromatography using 30 g of silica and eluting with dichloromethane/methanol (92/8) led to 240 mg of a beige powder (50% yield). Mp = 142 °C. ^{1}H NMR (200.13 MHz; $CDCl_3$): δ 9.17 (1H, dd, H_2 or H_9, J = 4.3; 1.5 Hz), 9.10 (1H, dd, H_9 or H_2, J = 4.3; 1.5 Hz), 8.38 (1H, dd, H_4 or H_7, J = 8.3; 1.5 Hz), 8.15 (1H, dd, H_7 or H_4, J = 8.3; 1.5 Hz), 7.63. (1H, dd, H_3 or H_8, J = 8.3; 4.3 Hz), 7.57 (1H, dd, H_8 or H_3, J = 8.2; 4.3 Hz), 7.56 (1H, s, H_6), 3.72 (2H, t, H_{14}, J = 6.2 Hz), 3.15 (2H, t, H_{11}, J = 7.2 Hz), 1.59−1.97 (4H, m, H_{12}, H_{13}). ^{13}C NMR (50.32 MHz; $CDCl_3$): δ 149.6, 146.5, 145.6, 137.0, 135.3, 132.2, 128.3, 128.0, 123.1, 122.7, 62.3, 32.6, 32.3, 26.4. IR (KBr): ν_{CHaro} = 3041 cm^{-1}, $\nu_{CH\ alkyl}$ = 2931, 2908 cm^{-1}, $\nu_{C=C\ aro}$ = 1563, 1510, 1425 cm^{-1}, δ_{OH} = 1378 cm^{-1}, ν_{C-O} = 1072 cm^{-1}, δ_{CHaro} = 744 cm^{-1}; UV/vis (CH_2Cl_2): 232 (39800); 268 (28300). Anal. Calcd for $C_{16}H_{16}N_2O_1$, 0.125 H_2O: C, 75.49; H, 6.43; N, 11.00%. Found: C, 75.62; H, 6.21; N, 10.83%.

5-(butanal)-1,10-phenanthroline **3**. To 0.9 g of iodoxybenzoic acid (IBX) (3.2 mmol) dissolved in 20 mL of DMSO dried on CaH_2 was dropwise added under an inert atmosphere 10 mL of a solution of 0.4 g of 5-(butan-1-ol)-1,10-phenanthroline (1.6 mmol) in DMSO. The reaction mixture was then stirred for a night, before being poured in a mixture of iced water and dichloromethane. The white precipitate formed was filtred. The two phases were separated and the organic layer was washed twice with brine, then washed several times with cold water to obtain 200 mg of a brown powder (50% yield). Mp = 83 °C. ^{1}H NMR (200.13 MHz; $CDCl_3$): δ 9.84 (1H, s, H_{14}), 9.18 (1H, dd, H_9 or H_2, J = 4.3; 1.6 Hz), 9.13 (1H, dd, H_2 or H_9, J = 4.3; 1.5 Hz), 8.49 (1H, dd, H_4 or H_7, J = 8.3; 1.5 Hz), 8.15 (1H, dd, H_7 or H_4, J = 8.3; 1.5 Hz), 7.67. (1H, dd, H_3 or H_8, J = 8.3; 4.3 Hz), 7.60 (1H, dd, H_8 or H_3, J = 8.2; 4.3 Hz), 7.59 (1H, s, H_6), 3.15 (2H, t, H_{13}, J = 7.4 Hz), 2.62 (2H, t, H_{11}, J = 7.1 Hz), 2.12 (2H, quint, J = 7.1 Hz). ^{13}C NMR (50.32 MHz; $CDCl_3$): δ 201.7, 149.9, 136.2, 135.5, 132.3, 128.3, 127.9, 125.4, 123.2, 122.9, 43.4, 31.8, 22.5. IR (KBr): $\nu_{CH\ aro}$ = 3070, 3026 cm^{-1}, $\nu_{CH\ alkyl}$ = 2948, 2918 cm^{-1}, $\nu_{C=O\ ald}$ = 1714 cm^{-1}, $\nu_{C=C\ aro}$ = 1565, 1510, 1421 cm^{-1}, $\delta_{CH\ aro}$ = 740 cm^{-1}. UV/vis (CH_2Cl_2): 212 (20200); 232 (37700); 268 (26300). Anal. Calcd for $C_{16}H_{14}N_2O_1$, 1.5 H_2O: C, 69.29; H, 6.17; N, 10.10%. Found: C, 68.91; H, 5.33; N, 9.75%.

5-(propyl-1-butan-1-imine)-1,10-phenanthroline **4**. 70 mg of the aldehyde **3** (0.28 mmol) and 41 mg propylamine (0.69 mmol, 2.5 equivalents) in 4 mL ethanol with molecular sieves (4 Å) were refluxed for 48 h. After filtration at room temperature, the solution was evaporated and dried. Thirty milligrams of the product were obtained in a mixture with 20% propylamine. ^{1}H NMR (200.13 MHz; $CDCl_3$): δ 9.16 (1H, dd, J = 4.3; 1.8 Hz); 9.12 (1H, dd, J = 4.3; 1.8 Hz); 8.50 (1H, dd, J = 8.7; 1.7 Hz); 8.16 (1H, dd, J = 8.7; 1.7 Hz); 7.35−7.75 (4H); 3.20−3.30; 3.15−3.30 (2H, m); 2.86 (t, 2H, 7.2 Hz); 2.05−2.15 (m, 2H); 1.55−1.70 (4H, m); 0.90−1.00 (3H,m). ^{13}C NMR (50.32 MHz; CD_2Cl_2): δ 163.8; 149.8; 141.00; 140.0; 137.4; 135.38; 133.4; 132.0; 128.3; 125.3; 123.2; 122.8; 63.1; 32.25; 32.0; 29.4; 28.0; 24.4; 12.0.

5-(butyl-1-butan-1-imine)-1,10-phenanthroline-(trichloro)Eu(I-II) complex **5**. Twenty milligrams (0.069 mmol, 2 equivalents) of **4** and 9 mg (0.035 mmol) of $EuCl_3$ in 3 mL of ethanol were refluxed for one night under an inert atmosphere. Filtration at room temperature of the reactional mixture gave 20 mg of a beige compound (69% yield). Anal. Calcd for $EuC_{44}H_{62}N_6Cl_3O_4$ (for $EuC_{38}H_{42}N_6Cl_3.1H_2O$, 3EtOH): C, 52.99; H, 6.26; N, 8.43; Eu 15,23%. Found: C, 52.77; H, 4.64; N, 8.80; Eu 14.79%.

LUS-1. LUS was prepared as follows:[68,69] 15.5 g of Ludox (0.26 mol) was added to 2 g of sodium hydroxide (5 × 10^{-2} mol) in

(67) Dess, D. B.; Martin, J. C. *J. Am. Chem. Soc.* **1991**, *113*, 7277–7287.
(68) Bonneviot, L.; Morin, M.; Badiei, A. Patent WO 01/55031 A1, 2001.
(69) Reinert, P.; Garcia, B.; Morin, C.; Badiei, A.; Perriat, P.; Tillement, O.; Bonneviot, L. *Stud. Surf. Sci. Catal.* **2003**, *146*, 133–136.

deionized water (50 mL) and then stirred at 313 K until clear (about 24 h). A second solution of hexadecyltrimethylammonium *p*-toluenesulfonate (CTATos) (2.5 g) in deionized water (90 mL) was stirred for 1 h at 333 K. The first solution was dropwise added to the second one then stirred at 333 K during 2 h. The resulting sol−gel was heated in an autoclave at 403 K during 20 h. After filtration and washing with deionized water (approximately 300 mL), the as-synthesized solid was dried at 353 K. Elemental anal. LUS-1: C(32.7%), H(6.7%), N(2.0%), S(0.4%), weight loss at 1273 K (49.3%). BET (Brunauer−Emmett−Teller method) surface area of 930 m^2 was obtained after solvent extraction and vacuum treatment at 423 K for 24 h.

Partial Extraction: LUS-PE. Five grams of as-made material LUS-1 was solubilized in technical ethanol (120 mL) and stirred at 313 K for a few minutes, and then 5.1 mL of hydrochloric acid 1 mol L^{-1} (standard from Acros company) was added. The mixture was stirred at 313 K for 1.5 h, then filtered and washed with technical ethanol (3 × 70 mL) and technical acetone (2 × 50 mL), and dried at 353 K for one night. Three grams of partially extracted silica was obtained. Anal. found for LUS-PE: C(16.6%), H(3.7%), N(0.7%), weight loss at 1273 K (18.5%).

Partial Silylation: LUS-PS. Three grams of partially extracted silica LUS-PE were placed in a two-neck round-bottom flask in order to be dried at 403 K during 1 h, first under an argon flow and then under a vacuum during 3 h. Back to room temperature, cyclohexane (100 mL) and hexamethyldisilazane HMDSA (20 mL) were added to the flask, and the mixture was stirred at room temperature for 1 h and then refluxed for 17 h. The mixture was filtered; washed with cyclohexane (3 × 70 mL), technical ethanol (3 × 70 mL), and acetone (50 mL); and dried at 353 K for 1 h. All these steps were repeated twice followed by an overnight drying at 353 K, leading to 3 g of partially silylated silica LUS-PS. Anal. found for LUS-PS: C(17.1%), H(3.7%), N(0.5%), weight loss at 1273 K (19.1%).

Extraction of Silica: LUS-PS-E. Three grams of partially silylated silica LUS-PS was dissolved in technical ethanol (180 mL), cooled at 273 K, and stirred at room temperature; 1.1 equiv. of hydrochloric acid 1 mol L^{-1} was slowly added. The mixture was stirred for 1 h at 273 K, and then filtered, washed with technical ethanol (3 × 70 mL) and acetone (2 × 50 mL), and dried at 353 K for one night, leading to around 2.5 g of extracted silica LUS-PS-E. Anal. Found for LUS-PS-E: C(5.9%), H(2.0%), N(<0.10%), weight loss at 1273 K (11.5%).

Aminopropyl Functionalization: LUS-PS-AP. LUS-PS-E (2 g) was placed in a round-bottom, two-neck flask and dried at 403 K for 1.5 h under nitrogen flow and then 2 h under a vacuum. The solid was solubilized in 50 mL of toluene. Five mL aminopropyltriethoxysilane (2.9 x10^{-2} mol) was added under nitrogen flow. The mixture was stirred at room temperature for 1 h and refluxed for 17 h. The obtained product was washed with toluene (3 × 40 mL), technical ethanol (3 × 40 mL), and acetone (2 × 30 mL). The bifunctionalized silica was dried at 353 K, leading to 2 g of LUS-PS-AP. Anal. found for LUS-PS-AP: C(10.2%), H(2.6%), N(1.03%), weight loss at 1273 K (11.5%). This material has been used to synthesize both material LUS-PS-Phen and two reference materials obtained by impregnation of either $EuCl_3$ or $Eu(Phen)_2Cl_3$, 3 H_2O on it (see the Supporting Information).

Reaction of Grafted Amine with 5-Butanal-Phen: LUS-PS-Phen. 5-butanal-Phen (98 mg) was solubilized in 30 mL of dry dichloromethane. In parallel, 0.32 g of LUS-PS-AP was placed in a round-bottom, two-neck flask, where 10 mL of dry dichloromethane was added. The 5-Butanal-Phen solution was added to the flask containing the solid. The mixture was stirred 2 h at room temperature and then 3 days at reflux. The obtained product was washed with dry dichloromethane (4 × 30 mL) and acetone (2 × 30 mL), leading to 0.35 g of bifunctionalized silica LUS-PS-Phen. Anal. Found for LUS-PS-Phen: C(19.0%), H(2.8%), N(2.4%), weight loss at 1273 K (24.0%).

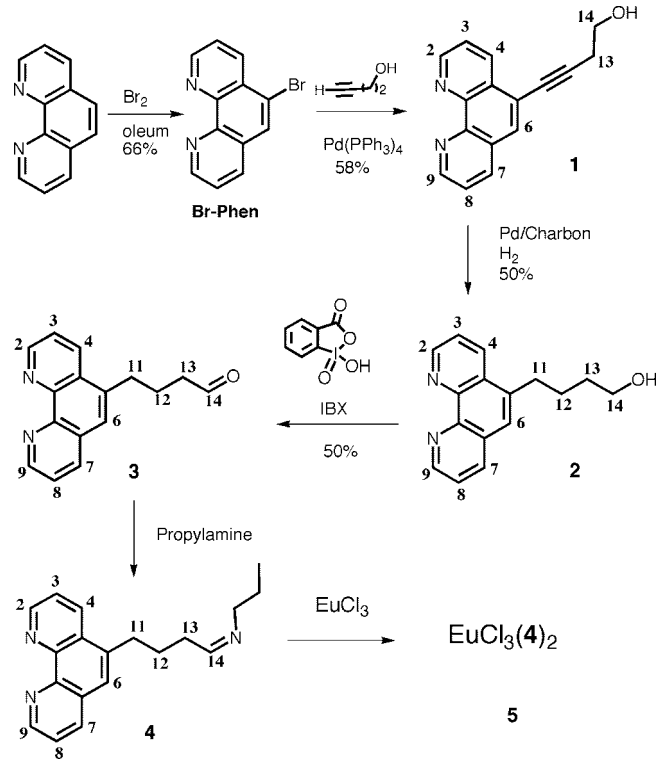

Figure 1. Synthetic procedure for compounds **3**, **4**, and **5** (general atom numbering is given for NMR description in the experimental section).

Reaction of Grafted Phenanthroline Ligand with $EuCl_3$: LUS-PS-Phen-Eu. To 100 mg of silica LUS-PS-Phen suspended in 15 mL of absolute ethanol was added a solution of 5.2 mg of $EuCl_3$ (2 × 10^{-5} mol) in 5 mL of EtOH. The reaction mixture was stirred under reflux and inert atmosphere for 48 h before being filtered; 98 mg of a beige powder was obtained. Anal. Found for LUS-PS-Phen-Eu: C(16.4%), H(2.7%), N(1.9%), Eu(1.8%), weight loss at 1273 K (23.1%). Other materials with a different Eu loading were prepared according to the same recipe. The relationship between the Eu concentration in solution and the Eu loading in the materials is depicted in Figure S1 of the Supporting Information.

Results and Discussion

LUS (Laval University Silica) has been used as mesostructured porous silica[68,69] then, according to the molecular stencil patterning approach (MSP),[45] sequential surface bifunctionalization of the porous material has been performed grafting first trimethylsilyl groups (TMS) and second aminopropylsilyl (APS) moieties using hexamethyldisilazane (HDMSA) and aminopropyltriethoxysilane (APTES) as organosilane reagents, respectively. A butanal derivative of the 1,10-phenanthroline (**3**, see Figure 1), which is a ligand specific to enhance the luminescence properties of Eu(III), has been designed to react selectively with the grafted APS moieties. The 1,10-phenanthroline derivative has been synthesized according to a synthetic route presented in Figure 1. 5-(But-3-yn-1-ol)-1,10-phenanthroline **1** was obtained according to a Sonogashira coupling reaction catalyzed by

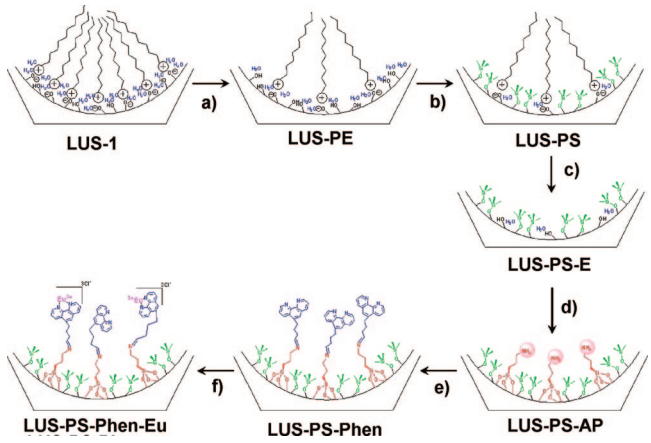

Figure 2. Steps of material synthesis from "as-made" LUS to bifunctionalized solid: (a) partial acidification, (b) partial trimethylsilylation, (c) total extraction, (d) grafting of 3-aminopropyltriethoxysilane, (e) reaction of grafted amino function and 5-(butanal)-1,10-phenanthroline **3**, (f) Eu(III) incorporation and complexation.

$Pd(PPh_3)_4$, starting from 5-bromo-1,10-phenanthroline[70] and the commercially available alkynol. Reduction with H_2 led to the corresponding alcohol **2** and its oxidation with the Dess-Martin like reactant IBX,[71] allowed the obtention of the desired aldehyde **3** with 50% yield. After metalation using $EuCl_3$ by default, several techniques were applied to check the integrity of the mesostructured porous silica support, the distribution of Eu in the material and the coordination of the latter. In parallel, the reaction of **3** with butyl-1-amine led to a novel imine molecular compound **4** (Figure 1). Its europium adduct **5**, with $EuC_{38}H_{42}N_6Cl_3 \cdot 1H_2O$, 3EtOH as empirical formula, was synthesized from compound **4** by mere metalation with 0.5 eq. of $EuCl_3$ (total yield of ca. 10% starting from **1**). Their physical and chemical properties were studied in comparison with their grafted analogues.

Evolution of the Inorganic Porous Matrix. Compound **3** was reacted with an organo-modified mesostructured porous silica (LUS-PS-AP), the characteristics of which are described in the following. In the first step, mesostructured silica LUS-1 was prepared in basic conditions in the presence of a cationic surfactant as structure directing agent (cetyltrimethylammonium *p*-toluenesulfonate, CTATos).[68,69] This silica is characterized by a 2D hexagonal periodic structure (*P6/m* symmetry point group), which is related to the MCM-41 structure,[72,73] as seen in the XRD pattern at low diffraction angles (Figure S2 in the Supporting Information). In a second step, the surface was prepared for bifunctionalization using the MSP approach. A controlled amount (ca. 75%) of the structure-directing agent (CTA^+) was removed by an titrated HCl ethanol solution leading to the partially extracted material denoted as for LUS-PE (Figure 2a). The grafting of TMS functions on the available surface silanol groups was then performed using an excess of HMDSA. This led to a partially silylated material, LUS-PS (Figure 2b). Before reacting APTES with the partially silylated silica, the remaining surfactant was carefully extracted with HCl ethanol solution at 273 K (LUS-PS-E). One and one-tenths equivalents of acid relative to surfactant present in the silica was used. Classical conditions of the grafting procedure were applied to introduce the APS tether leading to LUS-PS-AP. This solid was then reacted for 3 days in dichloromethane with compound **3** in refluxing conditions. The obtained LUS-PS-Phen was metalated for 24 h under reflux in absolute ethanol via treatment with 0.4 equiv. of $EuCl_3$ relative to the 1,10-phenanthroline moieties. The XRD powder investigation reveals a clear retention of the hexagonal array of the channel with neither change of line width nor of a_0 parameter. This is consistent with a long-range order maintained throughout the whole sequence of reactions. Nonetheless, a higher intensity of the XRD diagram is expected for a higher contrast between the silica wall and the channel atom occupancy.[47] Consistently, when the surfactant was totally removed, the intensity was at the highest and decreased progressively after each step of the synthesis reaching an intensity close to that of the material full of surfactant (spectrum not provided here). In parallel, the pore volume and the pore size were measured from the nitrogen adsorption−desorption isotherms (Figure S3 in the Supporting Information) for the LUS-PS-Phen-Eu and the parent material LUS-1. Both exhibit similar isotherms of type(IV) according to the IUPAC nomenclature,[74] which is also characteristic of such mesostructured porous materials.[68,69,75] The total pore volume measured at $P/P_0 = 0.98$, decreases from 0.96 cm^3/g in the extracted LUS down to 0.39 cm^3/g in LUS-PS-Phen-Eu (Table 1). In comparison, the volume is reduced down to 0.71 and 0.48 cm^3/g after full coverage by trimethylsilyl groups and butylsilane groups, respectively.[76] Note that the latter function should affect the pore volume like the APS tethers. The actual value then appears to be consistent with a mere pore filling by the organic functions (TMS and APS tether) and the europium complexes. Concomitantly, the surface is reduced from 1030 to 580 $m^2\ g^{-1}$. In addition, the capillary condensation occurring in a narrow range of pressures ($P/P_0 = 0.3-0.4$) shifts toward a lower range of pressures ($P/P_0 = 0.2-0.3$), consistent with a pore size reduction of about 0.6 nm. Nonetheless, a channel clearance of at least 2.4 nm according to BJH analysis (Barret−Joyner−Halenda) or 3.1 nm according to BdB analysis is maintained in LUS-PS-Phen-Eu (Table 1).

Table 1. Textural Properties of LUS-1 and LUS-P S-Phen-Eu

material	unit-cell parameter $\bar{a}$ (nm)[a]	BET surface area ($m^2\ g^{-1}$)[b]	porous volume[c] (mL g^{-1})	pore diameter (nm)[d]
LUS-1	4.6	1030	0.96	3.0
LUS-PS-Phen-Eu	4.8	580	0.39	2.4

[a] $\bar{a} = 2d_{100}/\sqrt{3}$. [b] BET: Brunauer−Emmett−Teller method. [c] Total pore volume measured at $P/P_0 = 0.98$. [d] Using the BJH (Barret−Joyner−Halenda) method; note that BdB (Broekhoff and de Boer) method provides larger pore diameter of 3.7 (top) and 3.1 (bottom) nm.

(70) Hissler, M.; Connick, W. B.; Geiger, D. K.; McGarrah, J. E.; Lipa, D.; Lachicotte, R. J.; Eisenberg, R. *Inorg. Chem.* **2000**, *39*, 447–457.
(71) Dess, D. B.; Martin, J. C. *J. Am. Chem. Soc.* **1991**, *113*, 7277–7287.
(72) Kresge, C. T.; Leonowicz, M. E.; Roth, W. J.; Vartuli, J. C.; Beck, J. S. *Nature* **1992**, *359*, 710–712.
(73) Beck, J. S.; Vartuli, J. C.; Roth, W. J.; Leonowicz, M. E.; Kresge, C. T.; Schmitt, K. D.; Chu, C. T. W.; Olson, D. H.; Sheppard, E. W.; McCullen, S. B.; Higgins, J. B.; Schlenker, J. L. *J. Am. Chem. Soc.* **1992**, *114*, 10834–10843.
(74) Sing, K. S. W.; Everett, D. H.; Haul, R. A. W.; Moscow, L.; Pierotti, R. A.; Rouquerol, J.; Siemieniewska, T. *Pure Appl. Chem.* **1985**, *57*, 603–619.
(75) Lin, L.-P.; Lu, S.-G.; Lu, S.-Z. *Polyhedron* **1996**, *15*, 4069–4077.
(76) Antochshuk, V.; Jaroniec, M. *Chem. Mater.* **2000**, *12*, 2496–2501.

Table 2. Quantification of Chemical Species from Elemental Analysis and IR Spectra Reported in Mole Ratio vs Framework Silicon, Si_{inorg}

material	TMS[a,b] ± 10%	APS[a] ± 10%	Phen[a] ± 10%	Eu ± 5%
LUS-PS	0.19 (83)			
LUS-PS-AP	0.15 (65)	0.120[c](52)		
LUS-PS-Phen	0.15 (65)	0.034[d](15)	0.034 (15)	
LUS-PS-Phen-Eu	0.13 (57)	0.000[d](0)	0.032 (14)	0.0090[e]

[a] Values in parentheses for function surface coverage (see text). [b] Determined from integration of the IR peak at 850 cm^{-1} and normalized to the peak intensity at 450 cm^{-1} (see text). [c] Determined from elemental analysis (EA) of N. [d] Determined from EA taking into account $C/N = 6.66$ for the entire 1,10-phenanthroline-imino moiety and $C/N = 3$ for APS groups. [e] Corresponds to Eu/Si_{tot} = 0.12 in mmol g^{-1} (see Table S1 in the Supporting Information).

Therefore, XRD and N_2 adsorption−desorption analysis are consistent with no structure collapse and a mere pore filling by grafted and derivatized organic functions through the various steps of the synthesis. This allows us to rationalize the functionalization process as limited to surface modification only, excluding any rearrangement of the inorganic network.

Quantification of the Grafted Functions. The function loading is discussed in terms of molar ratio versus framework silicon, named here "inorganic silicon", Si_{inorg} (Table 2). By contrast, the "organic silicon", Si_{org}, stands for the silicon atoms of the grafted organosilanes, either TMS or APS fragments. Elemental analyses were used to quantify the amount of grafted organic functions. The amount of TMS has been measured independently using infrared spectroscopy by monitoring the intensity of the peak at 850 cm^{-1} that corresponds to one of the symmetric stretching modes of the [$SiOCH_3$] unit.[47] The silicon ($Si_{tot} = Si_{inorg} + Si_{org}$) content was determined by weight loss at 1273 K from TGA. There is 0.19 mol of TMS per mol of Si_{inorg} in LUS-PS, i.e., a coverage of 83% that decreases down to 0.15 mol of TMS per mol of Si_{inorg} in LUS-PS-AP after the grafting of APS tethers, i.e., 65% of TMS and 52% of APS coverages (Table 2).[77] According to the C/N ratio of the LUS-PS-Phen sample, the reaction of the grafted APS with the aldehyde functional group of compound **3** appears practically complete with no loss of grafted functions. The last step of metalation by Eu(III) chloride affect slightly the TMS loading (coverage decreasing from 65 to 57%). It is worth noting that europium was introduced by default, yielding to a retention of Eu/grafted Phen mole ratio of ca. 0.28 in the solid for 0.4 in the solution.

Electron Microscopy. The samples present different morphologies, long and short fibers most often packed together, as well as less-defined regions. For our demonstration, the focus was made on the best separated defined long fibers. Figure 3 shows two typical adjacent fibers with a diameter of about 80 nm and a length of around 2.2 μm. An adequate tilting to bring the bottom extremity of the fibers in Bragg position reveals the existence of periodically arranged tubes (see Figure S4 in the Supporting Information). In accordance with X-ray diffraction, the size of these tubes

(77) The molecular stencil patterning method operates with full coverage of the internal surface, which corresponds to 0.23 TMS group per silicon (molar ratio), i.e., about 2 functions per nm^2. Therefore, there is about one silanol group unreacted per nm^2 and likely unavailable for further functionalization. See refs 45 and 46.

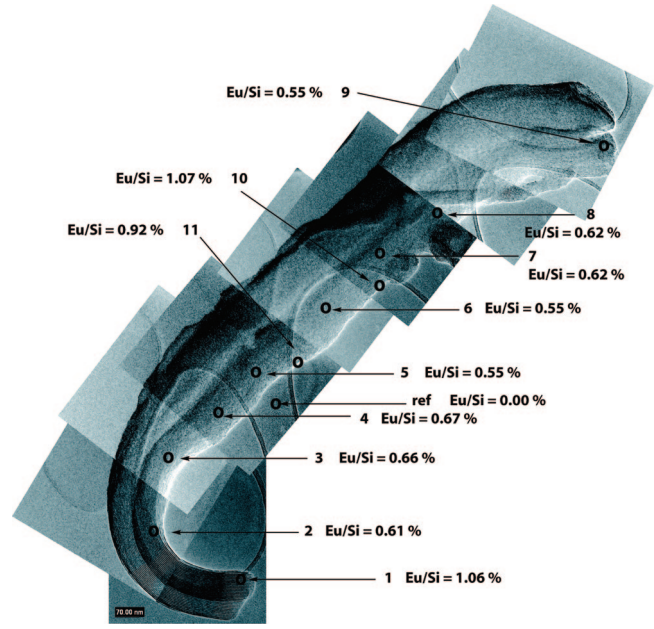

Figure 3. TEM micrograph of two adjacent fibers of a few micrometers. The Eu/Si atomic ratio has been determined by EDX along the fibers.

(pore and walls) is 3.56 ± 0.02 nm. At the very extremity of the fiber, EDX using a spot size of 1.5 nm (point 1, Figure 3) provides an atomic Eu/Si ratio of 1.06 ± 0.11%. This ratio decreases down to 0.61% after few tenths of a nanometer (point 2) to stabilize around this value inside the relative error of measurement error of ca. 10%, up to the other extremity for more than 2.5 μm (see Figure 3, points 2−9). Note that the absence of concentration gradient and the shape at this extremity (point 9) suggests that the fiber has been broken during the sample preparation for TEM observations, more likely during the ultrasonic dispersion treatment in ethanol. The EDX analysis on the side of the fiber (points 10 and 11) reveal also a concentration as high as at the extremity of the fiber (point 1). A global EDX analysis on these two adjacent fibers provides an Eu/Si mole ratio of 0.72 ± 0.07%. This is slightly below 0.90 at % obtained from chemical analysis but reasonably close to consider the actual concentration profile as characteristic of all the long fibers contained in the sample. For shorter fibers and less-defined parts of the samples, the Eu/Si mole ratio measured by EDX at a large scale is comprised between 0.86% and 0.98% in good concordance with chemical analysis (Table 2). Indeed, the extremities contain higher Eu loading than the bulk. Therefore, short objects will contribute for higher Eu loading than long fibers. However, it was not possible to obtain reasonable concentration profiles for small fibers because of the dense packing of such objects. All these data are consistent with a local Eu enrichment at the entrance of fibers and on their sides for a loading of ca. 1.0−1.2 at %, whereas in the interior after only few nanometers, the concentration is fairly constant for at least several micrometers all through the fiber. The TEM-EDX study using Eu(III) as a probe clearly demonstrates that MSP technique produces a homogeneous distribution of the APS tethers for several micrometers long in the nanochannels of the fibers. A slight europium enrichment at the channel entrance and at the external part of the fiber is reminiscent of a higher APS

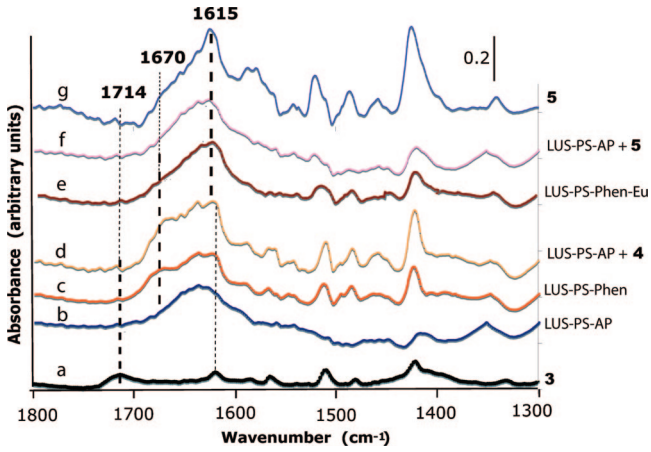

Figure 4. IR spectra of the materials and the molecular analogues of the grafted species in the range 1300−1800 cm^{-1}: (a) molecular compound **3** (see Figure 1), (b) TMS-APS bifunctional mesoporous silica (LUS-PS-AP), (c) same as in b after reaction with compound **3**, (d) composite IR spectrum obtained by adding spectrum of the imine molecular analogue **4** to spectrum b, (e) same as c after metalation by Eu(III), (f) composite IR spectrum obtained from adding spectrum of the Eu(III) molecular complex **5** to spectrum b, and (g) spectrum of the molecular complex **5**.

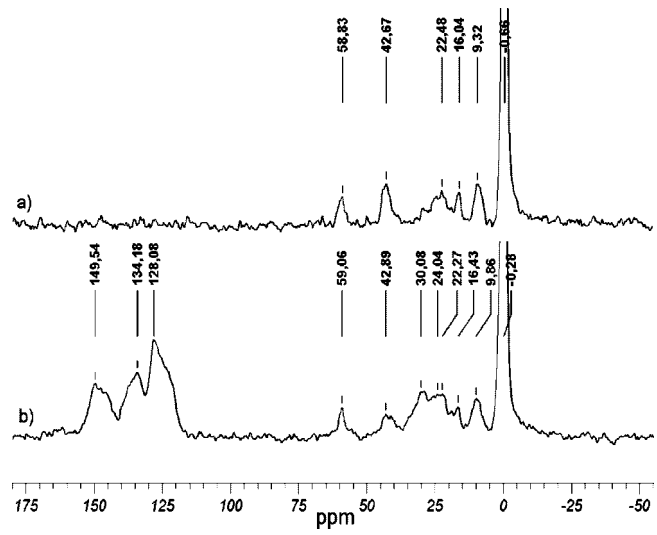

Figure 5. Solid-state ^{13}C CP-MAS NMR of (a) LUS-PS-AP and (b) LUS-PS-Phen; the peaks at 16 and 58 ppm are due to ethoxy groups. Peaks at about 9, 22, and 43 ppm are due to carbon in γ, β, and α position of the amino group, respectively. In LUS-PS-Phen, additional features appearing at about 25 ppm are attributed to the butyl-side arm of the 1,10-phenanthroline moiety derivative. The peaks between 123 and 160 ppm are assigned to aromatic carbons.

density at these locations. This is likely due to a higher displacement yield of the surfactant during the first step of MSP on the most solution accessible parts of the fiber. Such a weaker surface protection would indeed explain a higher grafting yield of APTES and therefore a higher Eu concentration at both external surface and channel entrances of the fibers.

Molecular Nature of the Grafted Ligand. After reaction of the LUS-PS-AP with **3**, the so-obtained LUS-PS-Phen is characterized by elemental analysis, NMR and by infrared spectroscopy, particularly in the range 1300−1800 cm^{-1} (see Figure 4). Concerning the matrix itself, a large band at 1630 cm^{-1} is assigned to the deformation vibration mode δ(H−O) of H_2O adsorbed on both external and internal surface of LUS-PS-AP. There is also a narrower but smaller band at 1410 cm^{-1} that may correspond to the N−C vibration mode of the APS group. As expected, 5-(butanal)-1,10-phenanthroline **3** prepared for reaction with APS tethers, exhibits much more peaks. The most characteristic of them is the stretching vibration mode $\nu_{C=O}$ at 1714 cm^{-1}, assigned to the aldehyde function. The other peaks at 1415, 1485, 1510, 1560, 1590, and 1610 cm^{-1}, are narrower and assigned to C═C and C═N stretching of the polycyclic frame of the 1,10-phenanthroline moiety. The latter are not observed on the spectrum of LUS-PS-AP but does appear on the spectrum of LUS-PS-Phen attesting for the presence of the polypyridyl ligand. The difference with compound **3** relies, on the one hand, in the absence of any peak in the region expected for an aldehyde group and in the apprearence of a new shoulder at 1670 cm^{-1} as expected for the stretching vibration mode $\nu_{C=N}$ of an imine function. This is consistent with a grafting according to a Schiff reaction as described in the synthesis of **4** (Figure 1). This assignment was confirmed by the fairly good match of the composite spectrum obtained by adding the IR spectra of LUS-PS-AP to the spectrum of the molecular imine compound **4**. This evidence the formation of the covalent grafting of the 1,10-phenanthroline ligand. The C and N elemental analysis combined with the quantitative IR control of the TMS coverage, allows calculation of the aminopropyl coverage at ca. 52% (i.e., 0.12 APS/Si_{inorg} mole ratio, Table 2). The analyses are consistent with about half conversion of aminopropyl groups into imine groups leading to 15% coverage in Phen ligand. Note that careful coverage calculations were performed taking into account the contribution of the silicon coming from the organosilanes (Si_{org}) because only inorganic silicon, Si_{inorg}, are useful here for correct coverage definition.[45,47]

Each step of the synthesis has also been characterized using ^{13}C CP-MAS NMR. The spectra of LUS-PS-AP and LUS-PS-Phen, namely before and after the grafting of the Phen moieties, are compared in Figure 5. The resonances at 9, 22, and 43 ppm are typical of the aliphatic carbons and are ascribed to the alkyl chains of both **3** and APS moieties. Note here that the complex structure of the peak at 22 ppm reveals the presence of a distribution of blocked conformation and likely partial protonation as expected for grafted APS moieties[78] (Figure 5a). In the range 115−160 ppm of the LUS-PS-Phen spectra (Figure 5b) new resonances consistent with aromatic carbon atoms is consistent with the presence of the polypyridyl ligand in the silica material. The Schiff reaction of grafting was performed in rather soft conditions that avoided TMS degrafting as already observed in during the grafting of APS moieties as usually observed with amino groups.[36]

Note that the formation of the imine was also evidenced in the molecular analogue **4**, by the disappearance of the resonance at 201.7 ppm ascribed in **3** to the aldehyde groups. Concomitantly, the appearance of a resonance at 163.8 ppm assigned to the imine function was observed. However, despite many efforts, the resonances for the imine group was not found on the NMR spectra of the grafted analogue LUS-PS-Phen, probably because of line broadening often observed in the material.

(78) Etienne, M.; Walcarius, A. *Talanta* **2003**, *59*, 1173–1188.

Nature of the Grafted Europium Complex in the 2D Hexagonal Silica. The reaction of LUS-PS-Phen with 0.4 equiv. of $EuCl_3$ per grafted Phen ligand yields to the LUS-PS-Phen-Eu material, with a Eu loading of 1.8%, i.e., a Eu/phen of 0.28 in the material (Table 2). This partial retention was systematically observed over a range of Eu concentration from 0.2 to 1.6 equiv., leading to a range of Eu/ratio varying from 0.14 to 0.8 (see Figure S1 in the Supporting Information). This shows that the complex is rather labile and the europium is partially removed when the solid is washed after the complexation reaction. Indeed, this was a prerequisite, to obtain a Eu distribution that properly map the ligand. In addition, note that the Eu metalation leads to the lost of the unreacted APS moieties as already observed with copper.[50]

The FT-IR spectra of LUS-PS-Phen-Eu exhibits significant evolution from the Eu free LUS-PS-Phen material. Again, the IR spectrum of the molecular equivalent compounds **5** was very useful to understand the band shift from 1670 to 1615 cm^{-1}. The feature at 1670 cm^{-1} assigned to the free imine molecule **4** disappeared in **5** while a well-defined peak at 1615 cm^{-1} appears as observed for the LUS-PS-Phen-Eu material. This strong red shift of $\nu_{C=N}$ in both cases (spectra e and g in Figure 4) is ascribed to a direct implication of the imine group in the coordination sphere of europium via the contribution of the lone electron pair of the nitrogen atom to coordination bonding.[79] (see discussion below and Figure S5 in the Supporting Information for a proposed molecular structure and coordination sphere of the Eu^{3+}). In addition, there is a new peak at 1580 cm^{-1} and a blue shift of the peak at 1510 up to 1520 cm^{-1}. The spectrum of LUS-PS-Phen-Eu, does not clearly exhibit the former type of peak, whereas the latter appears broader. Nonetheless, mathematical superimposition of the spectrum of LUS-PS-AP with the spectrum of compound **5** (Figure 4f) indeed matches well that of LUS-PS-Phen-Eu and reproduces the changes described above for the molecular analogues.

The luminescence spectrum of the $Eu(Phen)_2Cl_3(H_2O)_3$[80] complex consists of 5 sets of sharp lines due to the $^5D_0 \rightarrow {}^7F_J$ transitions with $J = 0-4$ arising at 579, 592, 613, 651, and 699 nm, respectively (see Figure 6).[81] The $^5D_0 \rightarrow {}^7F_{1-2}$ and $^5D_0 \rightarrow {}^7F_4$ transitions present at least 3 Stark components marked with arrows in Figure 6 and are the most sensitive to local-ligand field splitting. For $J = 0$, 2 or 4, the intensity of the $^5D_0 \rightarrow {}^7F_J$ transitions increases for lower symmetry of the coordination sphere. To the contrary, the intensity of the $^5D_0 \rightarrow {}^7F_{1,3}$ transitions that depends on the magnetic dipole transition, is insensitive to the surrounding environment. Therefore, a high value of R (intensity ratio of $^5D_0 \rightarrow {}^7F_2$ and of $^5D_0 \rightarrow {}^7F_1$ luminescence) suggests that the Eu^{3+} occupies a low-symmetry site, without an inversion center. In the present study, the strong similarity between spectra

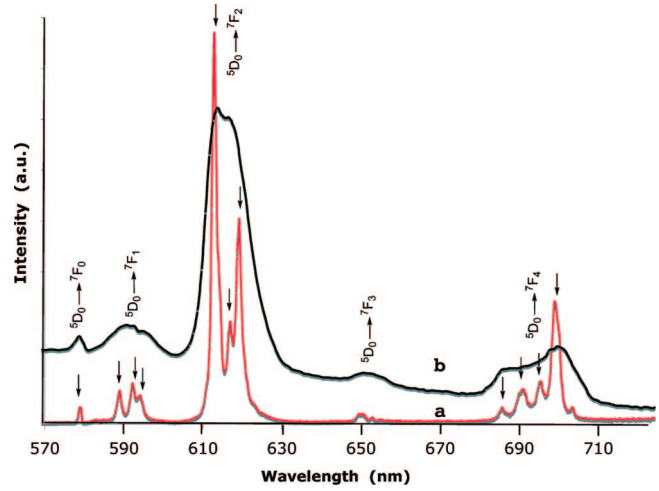

Figure 6. Room-temperature emission spectra of (a) complex $Eu(Phen)_2Cl_3(H_2O)_3$ and (b) LUS-Phen-Eu; arrows indicate the Stark components.

of both molecular complex $Eu(Phen)_2Cl_3(H_2O)_3$ and LUS-PS-Phen-Eu, with R values of 7.4 and 8.0, respectively, suggests a very similar environment symmetry for the europium cations in both systems. In addition, the $^5D_0 \rightarrow {}^7F_0$ transition characterized by a single peak for a single species is a convenient fingerprint to probe site distribution. In LUS-PS-Phen-Eu, the single line observed for this transition is consistent with a single type of site. Note that the molecular complex $Eu(Phen)_2Cl_3 \cdot 3H_2O$ directly impregnated at about the same metal loading on LUS-PS-AP than in LUS-PS-Phen-Eu (1.6 and 1.8% weight, respectively, and the preparation method in the Supporting Information) exhibits a similar fluorescence profile (see Figure S6 in the Supporting Information). However, the fluorescence is five times less intense than in presence of the grafted Phen ligand. When the impregnation is made using the nonfluorescent $EuCl_3$ salt on LUS-PS-AP (no Phen present, see preparation in the Supporting Information), the material exhibits a fluorescence, still 2.5 times less intense than LUS-PS-Phen-Eu (see Figure S6 in the Supporting Information). However, in the absence of the 1,10-phenanthroline moiety, the fluorescence profile is different (less intense $^5D_0 \rightarrow {}^7F_4$ transitions in comparison with the main fluorescent transitions $^5D_0 \rightarrow {}^7F_2$ and a different intensity profile within the latter set of $^5D_0 \rightarrow {}^7F_2$ transitions (see Figure S6 in the Supporting Information).

The excitation spectrum in the solid state for molecular complex $Eu(Phen)_2Cl_3(H_2O)_3$ displays a maximum around 355 nm (Figure 7a) which can be attributed to the $\pi-\pi^*$ transitions of the phenanthroline moiety, also observed in the diffuse reflectance solid UV/vis spectrum of this compound (Figure 7, bottom). This band is observed in the excitation spectrum of LUS-PS-Phen-Eu (Figure 7b) superimposed with the absorption of the LUS matrix (Figure 7c), the latter being responsible of a weak and broad emission of the silica.

The lifetime measurement at room temperature (Figure 8) provides the decay of the $^5D_0$ luminescence measured at 613 nm and excited at 360 nm. A monoexponential function fits well this decay curve for a lifetime of ca. 0.53 ms. This shows that the grafted europium complexes all experience

(79) Examples in the literature concern mostly conjugated imino-groups (mostly iminopyridyl moieties), the red shift of which is often modest, ca. -20 cm^{-1}, and rarely as high as -50 cm^{-1}. The present case concerns a non-conjugated lone pair; it is therefore not surprising to observe a quite large shift of -55 cm^{-1}. Lappalainen, M.; Yliheikkilä, K.; Abu-Surrah, A. S.; Polamo, M.; Leskelä, M.; Repo, T. *Z. Anorg. Allg. Chem.* **2005**, *631*, 763–768.

(80) Li, H.; Fu, L.; Liu, F.; Wang, S.; Zhang, H. *New J. Chem.* **2002**, *26*, 674–676.

(81) Richardson, F. *Chem. Rev.* **1982**, *82*, 541–552.

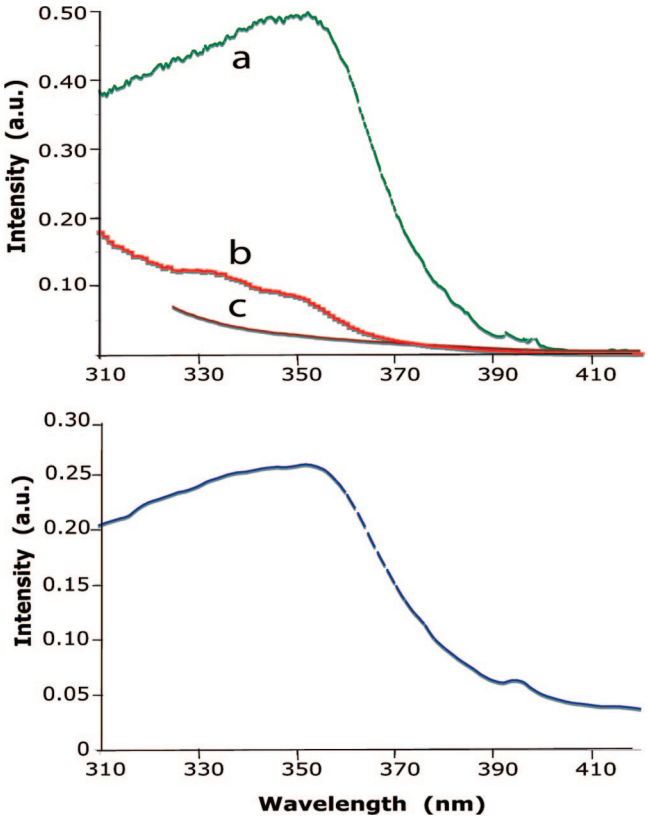

Figure 7. Room-temperature excitation spectra from emission at 613 nm (top) of (a) molecular complex $Eu(Phen)_2Cl_3(H_2O)_3$ in the solid state, (b) LUS-PS-Phen-Eu, and (c) pure LUS silica at 613 nm; diffuse reflectance UV−vis spectrum (bottom) of $Eu(Phen)_2Cl_3(H_2O)_3$ (same state as in a).

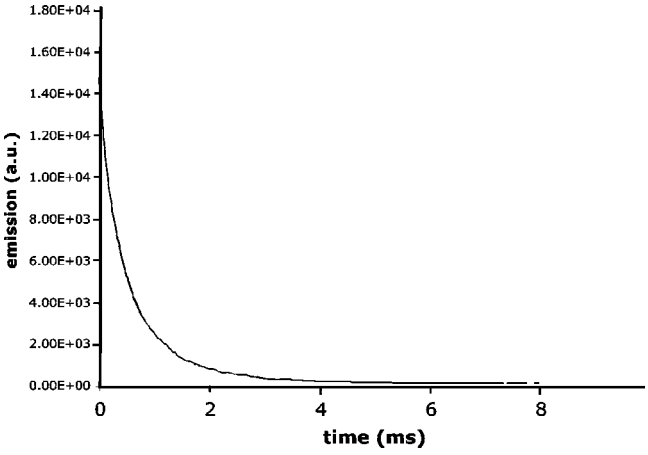

Figure 8. Luminescence time decay of LUS-PS-Phen-Eu material. Fitting of the experimental curve: $y = A_1\exp(-x/t_1) + y_0$, with $y_0 = 160 \pm 20$, $A_1 = 14500 \pm 100$, $t_1 = 0.529 \pm 0.007$, $R^2 = 0.994$.

similar decay rates, which is consistent with only one type of Eu site. The XRD structure of the molecular complex $Eu(Phen)_2Cl_3(H_2O)_3$ is not available and the coordination sphere of europium has been recently investigated by some of us, using among other techniques, EXAFS and density functional theory (DFT).[56] It appears that despite the presence of two Phen ligands in the stoichiometry, only one of them effectively participates to the first coordination sphere of Eu. By contrast, all the chloride ions and the water molecules are likely directly bound to Eu(III) leading to a neutral octacoordinated complex, $[Eu(H_2O)_3(Phen)Cl_3]Phen$. A similar case is observed in the neutral tris(*o*-aminobenzoate)(2,2-bipyridine)Eu complex, [Eu(*o*-ABA)$_3$bipy)]bipy, where only one of the two bipy molecules is effectively bound to Eu(III).[42] From elemental analyses, the $Eu(\mathbf{4})_2Cl_3\cdot H_2O\cdot$ 3EtOH formula can be proposed for **5**. Assuming the participation of the imino group to the Eu coordination sphere according to the significant C═N stretching frequency shift from 1670 to 1615 cm^{-1}, the iminobipyridyl function of **4** is likely to act as a tridentate ligand (see Figure S5 in the Supporting Information). Because Eu is usually 8- or sometimes 9-fold coordinated, there are two different options for **5** (see Figure S5 in the Supporting Information). There is no water nor ethanol in the coordination of europium with structure $[Eu(\mathbf{4})_2Cl_3]H_2O,3EtOH$ with a coordination of 9; this would imply the presence of one water and tree ethanol molecules in the outer sphere of coordination in the solid. The second option assumes an outer sphere molecule **4** like in the Phen analogue (see above) and a structure of type $[Eu(H_2O)(EtOH)_x(\mathbf{4})Cl_3]\mathbf{4},EtOH_{3-x}$ with a coordination state of 8 or 9 for $x = 1, 2$ (see Figure S5 in the Supporting Information). In the material LUS-PS-Phen-Eu, the grafted Eu species are likely to resemble that of the solid **5**. The imine complexation implies a folding of the side arm of the derivatized 1,10-Phen moieties on itself. Because a single tridentate **4** and 3 chloro ligands are expected to bind directly Eu(III), at least 2 positions are left to fill 8 coordination positions. At this point, it is not clear what are the ligand occupying these positions; it could be either water molecules from ambient air, residual ethanol used for washing the material, or residual surface silanol groups rendered available during the metalation step (Table 2). Anyhow, according to Stern−Volmer equation,[82−84] a rather "dry" coordination is expected to explain the slow luminescence decay observed here for the grafted europium species as compared to molecular complex $Eu_3Phen_2Cl_2.3H_2O$ (0.38 ms).[85] Consistently, TGA shows that LUS-PS-Phen-Eu is much more hydrophobic than LUS-PS-AP impregnated with $EuCl_3$ or with $Eu(Phen)_2Cl_3(H_2O)_3$ (water mass loss of 2.7, 9.1 and 3.6% weight below 120 °C, respectively, see Figure S7 in the Supporting Information).

Conclusion

In this study, 2D hexagonal templated silicas named LUS, structurally similar to the well-known MCM-41, have been used to test the so-called "molecular stencil patterning" (MSP) approach, for its capacity to generate both isolation of grafted surface functions and homogeneous dispersion inside the confined space of the channel on the micrometer scale of length. Here, the isolated functions were the aminopropylsilyl moieties (APS), whereas the diluting functions were the trimethylsilyl groups (TMS). The latter were introduced prior the former by reacting hexamethyldisilazane with surface silanol groups left accessible by partial extraction of the templating surfactant of an as-made mesostruc-

(82) Horrocks, W.; De, W.; Sudnick, D. R. *Acc. Chem. Res.* **1981**, *14*, 384–392.
(83) Bünzli, J.-C. G.; Vuckovic, M. *Inorg. Chim. Acta* **1984**, *95*, 105–112.
(84) Beeby, A.; Clarkson, I. M.; Eastoe, J.; Faulkner, S.; Warne, B. *Langmuir* **1997**, *13*, 5816–5819.
(85) Guo, X.; Fu, L.; Zhang, H.; Carlos, L. D.; Peng, C.; Guo, J.; Yu, J.; Deng, R.; Sun, L. *New J. Chem.* **2005**, *29*, 1351–1358.

tured porous silica. For the sake of analytical investigation, Eu(III) ion was chosen as a molecular marker to localize the APS tethers. To optimize the luminescence yield of europium, we have specially designed and reacted a 1,10-phenanthroline possessing an aldehyde side arm, **3**, with the APS tethers according to the Schiff reaction. Metalation was then performed by mere contact with a solution of $EuCl_3$ in EtOH. The integrity of the 2D hexagonal array of the channels has been checked using XRD powder pattern and the pore filling by the molecular probe was attested by N_2 adsorption−desorption data. The Schiff reaction was found quantitative and the so-obtained grafted ligand was characterized using both IR and ^{13}C NMR. The metalation of the grafted imino-phenanthroline moieties by $EuCl_3$ was attested by chemical analysis, IR, and luminescence properties. It appears that the grafted phenanthroline moiety acts rather as a tridentate ligand on $EuCl_3$ like its molecular analogue compound **4**. However, the grafted europium complex shows some specificity in comparison to its molecular analogue **5** not fully resolved here. Anyhow, the labile nature of this complex ensures a mapping of the grafted aminopropyl moieties in the solid. The EDX-TEM investigation at a resolution of 1.5 × 1.5 nm show that the MSP technique is an efficient tool to homogeneously distribute grafted functions in the confined space of 1D nanochannels several micrometers long. However, there is still more to be done in order to better control the external surface chemistry of such porous materials leading to a "hybrid-material engineering".

Acknowledgment. Both CNRS and 'Région Rhône-Alpes' ('Thématique prioritaire' 301439201/E038131747/ENS2006) are acknowledged for their financial support. Sophie Nicolas is also acknowledged for her contribution to this work during her master internship.

Supporting Information Available: Powder X-ray diffractograms, nitrogen adsorption−desorption isotherms, TEM pictures, thermal gravimetric analysis, procedures for the preparation of materials and their characterization (PDF). This material is available free of charge via the Internet at http://pubs.acs.org.

CM802752R